# Selective Crystallization of Organic Semiconductors for High Performance Organic Field-Effect Transistors

**ARTICLE** *in* CHEMISTRY OF MATERIALS · OCTOBER 2009

Impact Factor: 8.35 · DOI: 10.1021/cm902594y



**9 AUTHORS**, INCLUDING:

Chong-an Di
Chinese Academy of Sciences
**109** PUBLICATIONS **3,727** CITATIONS
SEE PROFILE

Weiping Wu
University of Cambridge
**153** PUBLICATIONS **4,504** CITATIONS
SEE PROFILE

Yunlong Guo
Chinese Academy of Sciences
**116** PUBLICATIONS **3,716** CITATIONS
SEE PROFILE

Xiangnan Sun
CIC nanoGUNE Consolider
**32** PUBLICATIONS **550** CITATIONS
SEE PROFILE

CHEMISTRY OF MATERIALS
Article

*Chem. Mater.* **2009,** *21,* 4873–4879 4873
DOI:10.1021/cm902594y

# Selective Crystallization of Organic Semiconductors for High Performance Organic Field-Effect Transistors

Chong-an Di, Gui Yu, Yunqi Liu,* Yunlong Guo, Xiangnan Sun, Jian Zheng, Yugeng Wen, Weiping Wu, and Daoben Zhu*

*Beijing National Laboratory for Molecular Sciences, Institute of Chemistry, Chinese Academy of Sciences, Beijing 100190, P. R. China*

*Received June 26, 2009*

The patterning of an organic layer, a big challenge for organic field-effect transistors (OFETs), have recently received considerable attention. By using copper tetracyanoquinodimethane (Cu-TCNQ) modified copper electrodes with nanostructure, selective polycrystalline growth of organic semiconductors is achieved. For different organic semiconductors, varied ways for crystal growth are observed. The OFETs based on selectively deposited tetracyanoquinodimethane (TCNQ), rubrene, and copper phthalocyanine crystals are fabricated and exhibit good device performance. Rubrene devices exhibit maximum field-effect mobility up to 4.6 $cm^2/(V \cdot s)$ which is comparable to that of corresponding single crystal device. In addition, an organic inverter made of patterned rubrene and TCNQ exhibits a gain of 23. These results offer a general approach to the fabrication of high performance OFETs and organic circuits.

## Introduction

During the past decade, increasing interest has been focused on organic field-effect transistors (OFETs) and related functional materials. Up to now, many great achievements have been made.[1−10] Recently, special attention has been given to the application of OFETs in organic circuits. The patterning of organic layers is an important issue for the construction of organic circuits since it can decrease parasitic current paths (crosstalk) between neighboring devices, and results in a significant decrease in the "off" current.[11−16] As a result, various techniques are developed to pattern an organic active layer. Single crystal OFETs attract great attention because they provide an ideal model to understand the charge transport mechanism of organic semiconductors and exhibit high device performance.[17−21] Bao et al. reported many interesting results on the patterning of organic single crystals.[14−16,22,23] By the patterning of octadecyltriethoxysilane and carbon nanotubes, they achieved effective patterning of organic crystals and constructed corresponding OFETs. Besides, a lot of other achievements have been recently demonstrated by different groups.[24−26] These approaches represent novel routes toward integrated single crystal OFETs. However, many

*Corresponding authors. E-mail: liuyq@iccas.ac.cn, zhudb@iccas.ac.cn.

(1) Liu, J. Y.; Zhang, R.; Sauvé, G.; Kowalewski, T.; McCullough, R. D. *J. Am. Chem. Soc.* **2008**, *130*, 13167–13176.
(2) Fong, H. H.; Pozdin, V. A.; Amassian, A.; Malliaras, G. G.; Smilgies, D.; He, M. Q.; Gasper, S.; Zhang, F, X.; Sorensen, M. *J. Am. Chem. Soc.* **2008**, *130*, 13202–13203.
(3) Meng, H.; Sun, F.; Goldfinger, M. B.; Gao, F.; Londono, D. J.; Marshal, W. J.; Blackman, G. S.; Dobbs, K. D.; Keys, D. E. *J. Am. Chem. Soc.* **2006**, *128*, 9304–9305.
(4) Li, J.; Qin, F.; Li, C. M.; Bao, Q.; Chan-Park, M. B.; Zhang, W.; Qin, J.; Ong, B. S. *Chem. Mater.* **2008**, *20*, 2057–2059.
(5) Letizia, J. A.; Salata, M. R.; Tribout, C. M.; Facchetti, A.; Ratner, M. A.; Marks, T. J. *J. Am. Chem. Soc.* **2008**, *130*, 9679–9694.
(6) Yan, H.; Zheng, Y.; Blache, R.; Newman, C.; Lu, S. F.; Woerle, J.; Facchetti, A. *Adv. Mater.* **2008**, *20*, 3393–3398.
(7) Klauk, H.; Zschieschang, U.; Pflaum, J.; Halik, M. *Nature* **2007**, *445*, 745–748.
(8) Nakagawa, T.; Kumaki, D.; Nishida, J.-I.; Tokito, S.; Yamashita, Y. *Chem. Mater.* **2008**, *20*, 2615–2617.
(9) Zhang, M.; Tsao, H. N.; Pisula, W.; Yang, C. D.; Mishra, A. K.; Müllen, K. *J. Am. Chem. Soc.* **2007**, *129*, 3472–3473.
(10) Zaumseil, J.; Friend, R. H.; Sirringhaus, H. *Nat. Mater.* **2006**, *5*, 69–74.
(11) Park, S. Y.; Kwon, T.; Lee, H. H. *Adv. Mater.* **2006**, *18*, 1861–1864.
(12) Wang, Z.; Zhang, J.; Xing, R.; Yuan, J. F.; Yan, D. H.; Han, Y. C. *J. Am. Chem. Soc.* **2003**, *125*, 15278–15279.
(13) Shtein, M.; Peumans, P.; Benziger, J. B.; Forrest, S. R. *J. Appl. Phys.* **2003**, *93*, 4005–4016.
(14) Mannsfeld, S. C. B.; Briseno, A. L.; Liu, S. H.; Reese, C.; Roberts, M. E.; Bao, Z. N. *Adv. Funct. Mater.* **2007**, *17*, 3545–3553.
(15) Briseno, L.; Mannsfeld, S. C. B.; Ling, M. M.; Liu, S. H.; Tseng, R. J.; Reese, C.; Roberts, M. E.; Yang, Y.; Wudl, F.; Bao, Z. N. *Nature* **2006**, *444*, 913–917.
(16) Mannsfeld, S. C. B.; Sharei, A.; Liu, S.; Roberts, M. E.; Bao, Z. *Adv. Mater.* **2008**, *20*, 4044–4048.
(17) de Boer, R. W. I.; Stassen, A. F.; Craciun, M. F.; Mulder, C. L.; Molinari, A.; Rogge, S.; Morpurgo, A. F. *App. Phys. Lett.* **2005**, *86*, 262109.
(18) de Boer, R. W. I.; Gershenson, M. E.; Morpurgo, A. F.; Podzorov, V. *Phys. Stat. Sol. A* **2004**, *201*, 1302–1331.
(19) Sundar, V. C.; Zaumseil, J.; Podzorov, V.; Menard, E.; Willett, R. L.; Someya, T.; Gershenson, M. E.; Rogers, J. A. *Science* **2004**, *303*, 1644–1646.
(20) Menard, E.; Podzorov, V.; Hur, S.-H.; Gaur, A.; Gershenson, M. E.; Rogers, J. A. *Adv. Mater.* **2004**, *16*, 2097–2101.
(21) Menard, E.; Marchenko, A.; Podzorov, V.; Gershenson, M.; Fichou, D.; Rogers, J. A. *Adv. Mater.* **2006**, *18*, 1552–1556.
(22) Liu, S. H.; Briseno, A. L.; Mannsfeld, S. C. B.; You, W.; Locklin, J.; Lee, H. W.; Xia, Y. N.; Bao, Z. N. *Adv. Funct. Mater.* **2007**, *17*, 2891–2896.
(23) Liu, S. H.; Mannsfeld, S. C. B.; Wang, W. M.; Sun, Y. S.; Stoltenberg, R. M.; Bao, Z. N. *Chem. Mater.* **2009**, *21*, 15–17.
(24) Verlaak, S.; Steudel, S.; Heremans, P.; Janssen, D.; Deleuze, M. S. *Phys. Rev. B* **2003**, *68*, 195409.
(25) Lee, H. S.; Kim, D. H.; Cho, J. H.; Hwang, M.; Jang, Y.; Cho, K. *J. Am. Chem. Soc.* **2008**, *130*, 10556–1056.
(26) Virkar, A.; Mannsfeld, S.; Oh, J. H.; Toney, M. F.; Tan, Y. H.; Liu, G.; Scott, J. C.; Miller, R.; Bao, Z. *Adv. Funct. Mater.* **2009**, *19*, 1962–1970.


Published on Web 10/02/2009

challenges still remain. As an example, the size and shape of organic crystals are difficult to be controlled precisely.[23] It results in nonuniformity in size and shape of patterned crystals and brings on different channel width and thus great variation in device performance.[23] As a comparison, good uniformity can be obtained for thin film OFETs. Therefore, the patterning of organic thin films is another desirable subject. Liu et al. recently demonstrated their "dry-taping" approach toward patterning of pentacene thin films.[27] Despite effective thin film patterning; the device performances are much lower than that of single crystal devices. For thin film OFET, enlarging organic grains is a general way to improve device performance. Selective growth of large polycrystals thus might be a useful route to achieve high performance OFETs with a patterned active layer.

Source−drain (S−D) electrodes are important parts of OFETs. Both the work function of the S−D electrodes and electrode/organic layer interface condition affect the carrier injection and device performance dramatically.[28,29] A typical bottom gate OFET can be divided into top-contact and bottom-contact configurations. For the bottom contact devices, organic semiconductors are deposited after fabrication of the S−D electrodes. Therefore, the properties of the electrodes can influence deposition of the organic semiconductors. For example, modification of pentafluorobenzene thiol (PFBT) on gold electrodes facilitates the crystalline of 5,11-bis(triethylsilylethynyl) anthradithiophene.[30] The result indicates that the optimization of the S−D electrodes is an effective way to control the growth of the organic layer. In this paper, we report a novel approach to the fabrication of high performance OFETs based on selectively patterned organic polycrystals. When copper tetracyanoquinodimethane (Cu-TCNQ) modified Cu, an excellent electrode for many thin film OFETs,[28,29] serves as S−D electrodes, many organic crystals grow selectively near the electrodes. The paths for polycrystalline to grow are strongly related to properties of organic semiconductors. More interestingly, the device possesses high performance. These results offer a shortcut toward high performance OFETs with patterned organic polycrystals.

## Experimental Section

**The Source−Drain (S−D) Electrode Fabrication.** After the formation of 300 nm $SiO_2$ on $n^+$ doped Si, the copper S−D electrodes are deposited and patterned (lift off technique). The channel lengths are varied from 10 to 50 $\mu$m, while the channel width ($W$) is maintained at 1.4 mm. Then, the copper S−D electrodes are modified as follows.

**Modification of Cu Electrodes.** The vapor deposition modification of the Cu electrodes is carried out in a physical vapor transport (PVT) system with two different temperature zones. TCNQ powder and the substrates with the patterned Cu electrodes are placed at the high- and low-temperature zones, respectively, with temperature maintained at 170 and 90 °C. Then, Cu-TCNQ nanostructure is constructed on the Cu electrodes under pure Ar gas with flow rate of 25 sccm for 30 min. Finally, the Cu-TCNQ-modified Cu electrodes are used to induce selective growth of organic crystals.

**Selective Growth of TCNQ, Rubrene, and CuPc Crystals on Modified Electrodes.** The selective growths of TCNQ, rubrene, and CuPc crystals are carried out in a PVT system. Ar gas is used as the carrier. The organic semiconductor powders are placed at the high-temperature zone, while the substrates with modified Cu electrodes are placed at 2−7 cm away from the source of the organic semiconductors. Finally, the crystal deposition is performed. The source temperatures of TCNQ, rubrene, and CuPc are 175, 255, and 415 °C, respectively.

**Characterization of OFETs.** The characteristics of the OFETs were measured using a Keithley 4200-SCS semiconductor characterization system. All of the measurements were performed under ambient atmosphere at room temperature.

## Results and Discussion

Figure 1a shows the fabrication process of OFETs based on selectively patterned organic crystals. Before the patterning of organic crystals, the Cu S−D electrodes are modified with Cu-TCNQ crystals according to a previous report.[29] Cu-TCNQ nanowires vertical to the electrodes can be obtained (Figure 1b). Thereafter, the organic crystals grow selectively on the modified electrodes in a PVT system. Figure 1c shows the optical micrograph of selectively obtained TCNQ crystals. It can be clearly observed that the TCNQ polycrystals are only deposited on the premodified electrodes instead of bare $SiO_2$ surface. Therefore, both the shape and position of organic crystal can be controlled by the predeposited Cu electrodes. Note that, the evaporation zone temperatures, the substrates temperature, and crystal deposition time have to be strictly controlled during the deposition process. Higher or lower temperatures will result in poor quality of the crystal patterning. Compared with previous techniques, our method possesses the following advantages. In the previous reports, the introduction of a rough surface favors crystal nucleation,[14,15,22] but it could result in negative influence on the dielectric/organic layer interface. Since dielectric/organic layer interface is the most important one in OFETs and dominate the carrier transport, the relative poor dielectric/organic layer interface can lower the device performance dramatically. Herein, the rough electrodes are introduced to induce selective crystallization of organic semiconductors. Although the rough electrodes also influence the electrode/organic interface, the effect to the device performance might be smaller than that caused by the rough dielectric/organic layer interface. Therefore, the constructed devices might exhibit high device performances.

With the technique mentioned above, different crystals deposit near the modified electrodes. Figure 2 panels a−c

(27) Liu, S. H.; Becerril, H. A.; Lemieux, M. C.; Wang, W. M.; Oh, J. H.; Bao, Z. N. *Adv. Mater.* **2009**, *21*, 1217–1232.
(28) Di, C. A.; Yu, G.; Liu, Y. Q.; Xu, X. J.; Wei, D. C.; Song, Y. B.; Sun, Y. M.; Wang, Y.; Zhu, D. B.; Liu, J.; Liu, X. Y.; Wu, D. X. *J. Am. Chem. Soc.* **2006**, *128*, 16418–16419.
(29) Di, C. A.; Yu, G.; Liu, Y. Q.; Guo, Y. L.; Wu, W. P.; Wei, D. C.; Zhu, D. B. *Phys. Chem. Chem. Phys.* **2008**, *10*, 2302–2307.
(30) Gundlach, D. J.; Royer, J. E.; Park, S. K.; Subramanian, S.; Jurchescu, O. D.; Hamadani, B. H.; Moad, A. J.; Kline, R. J.; Reague, L. C.; Kirillov, O.; Richter, C. A.; Kushmerick, J. G.; Richter, L. J.; Parkin, S. R.; Jackson, T. N.; Anthony, J. E. *Nat. Mater.* **2008**, *7*, 216–221.

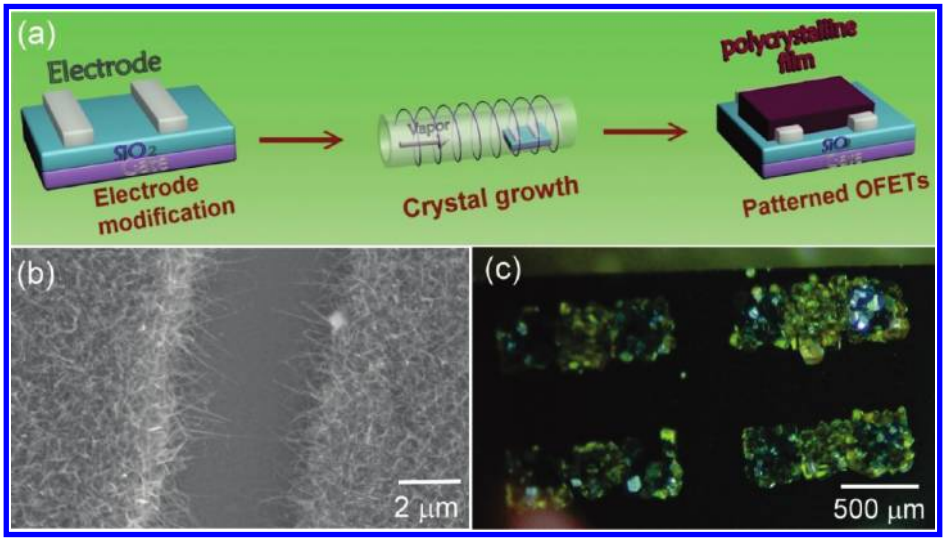


**Figure 1.** (a) Scheme of the fabrication process of OFETs based on the patterned organic crystals; (b) SEM images of the Cu-TCNQ modified Cu electrodes; (c) optical micrograph of OFETs with patterned TCNQ crystals on prepatterned Cu electrodes.

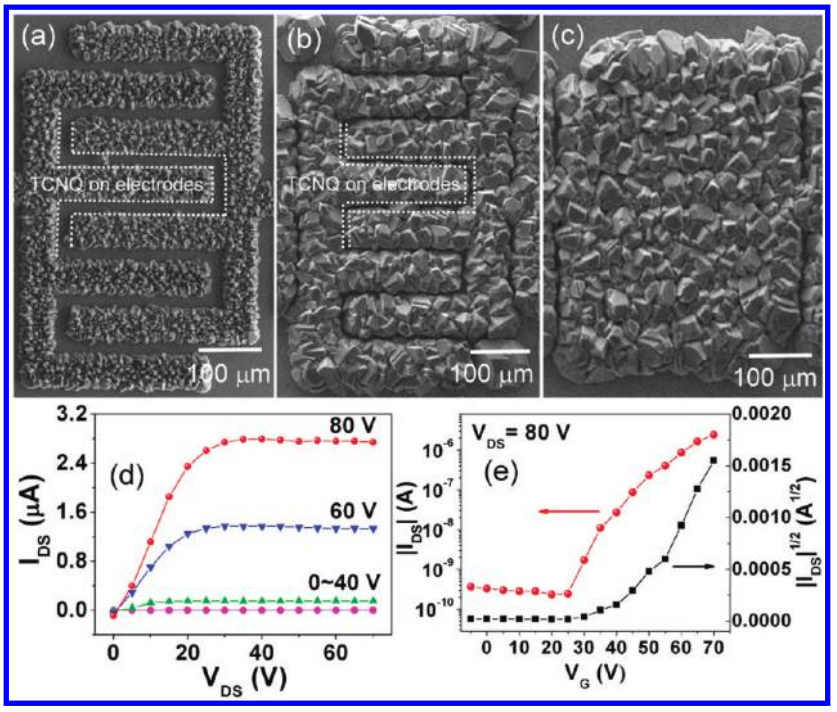


**Figure 2.** (a−c) SEM images of the patterned TCNQ crystals. The source temperature is kept at 175 °C, and the substrate temperature is maintained at (a) 85 °C for 10 min, (b) 85 °C for 40 min, (c) 85 °C for 60 min. (d) Output and (e) transfer characteristics of TCNQ devices.

show the SEM images of TCNQ crystals under different deposition conditions. Interestingly, the TCNQ crystals are located on the electrodes instead of $SiO_2$ region at the beginning stage of crystal deposition. In the following deposition process, the crystals grow larger and extend into the channel slightly. Even after deposition for 40 min, when the thickness of TCNQ crystals increases to a few micrometers, obvious $SiO_2$ channels can still be observed (Figure 2b). Fortunately, continuous TCNQ polycrystalline films formed once the deposition time went on to 60 min. The OFETs based on selectively deposited TCNQ crystals are thus constructed. Since the TCNQ crystals fill the electrodes region exactly, the $W/L$ is determined by the predeposited source−drain electrodes. Figure 2d and 2e show the output and transfer characteristics of obtained TCNQ devices. The devices are with n-type operation under ambient condition and exhibit good saturation characteristics. The field-effect mobility of $10^{-3}$ to $(2 \times 10^{-2})$ $cm^2/(V \cdot s)$ are extracted from transfer characteristics (Figure 2d and Table 1). These values are about 1−2 orders higher than the previous reported performance of patterned TCNQ devices.[15] Statistics of 40 devices with different channel length (10−50 $\mu$m) indicate that the devices exhibit moderate uniformity (Figure 3).

Rubrene crystals show different growth paths compared with TCNQ. The crystals are not only deposited on the S−D electrodes but also tend to grow in the channel (Figure 4). More interestingly, the crystals sizes

in the channel are much larger than those on the electrodes. Even rubrene single crystals across the whole channel

**Table 1. Detailed Performance of OFETs with Different Organic Semiconductors**

| | mobility ($cm^2/(V\cdot s)$) | $I_{on}/I_{off}$ | threshold voltage (V) |
|---|---|---|---|
| TCNQ | $10^{-3}$ to ($2 \times 10^{-2}$) | $(1-8) \times 10^4$ | 40 to 47 |
| rubrene | 0.2−4.6 | $10^5-10^6$ | −18 to −28 |
| CuPc | $(1-5) \times 10^{-3}$ | $(1-3) \times 10^4$ | −8 to −19 |

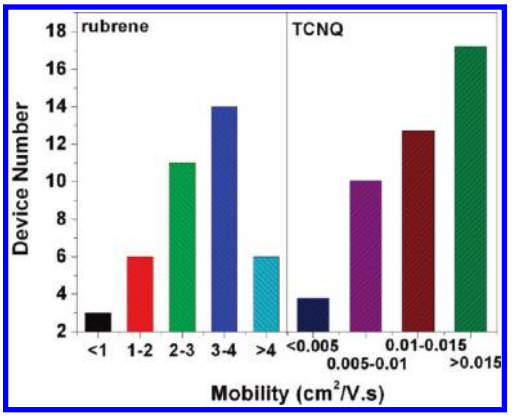


**Figure 3.** Device performances statistics of 40 OFETs-based rubrene and TCNQ crystals with channel length ranging from 10 to 50 $\mu$m.

are obtained (Figure 4a). As can been seen from Figure 4b,c,e, the size of rubrene crystals can reach 100−200 $\mu$m, which is large enough to construct single crystals FETs with channel length shorter than 50 $\mu$m. In fact, we fabricated short channel length OFETs made of rubrene single crystal array (Figure 3d). The rubrene-based device shows good output characteristics and shows high device mobility. A field-effect mobility higher than 1 $cm^2/(V\cdot s)$ can be obtained and with a maximum value of 4.6 $cm^2/(V\cdot s)$ (Table 1 and Figure 3). It is higher than that of rubrene polycrystalline film devices and is comparable with that of single crystal devices based on an $SiO_2$ dielectric layer.[15,31,32] The high device performance is ascribed to the following reason. First, although we fabricate the device with polycrystals, the crystal size is much larger than grains of general organic film and ever larger than channel length. Therefore, the boundary density is minimized and brings on high device performance comparable to that of single crystal based OFETs. Besides, we observed that the long sides of rubrene single crystals (*b*-axis) are almost vertical to the electrodes (see Figure 4). The packing direction facilitates carrier transport and ensures high carrier mobility.

As for CuPc, the crystals also grow on the modified electrodes at the beginning stage (Figure 5a). However,

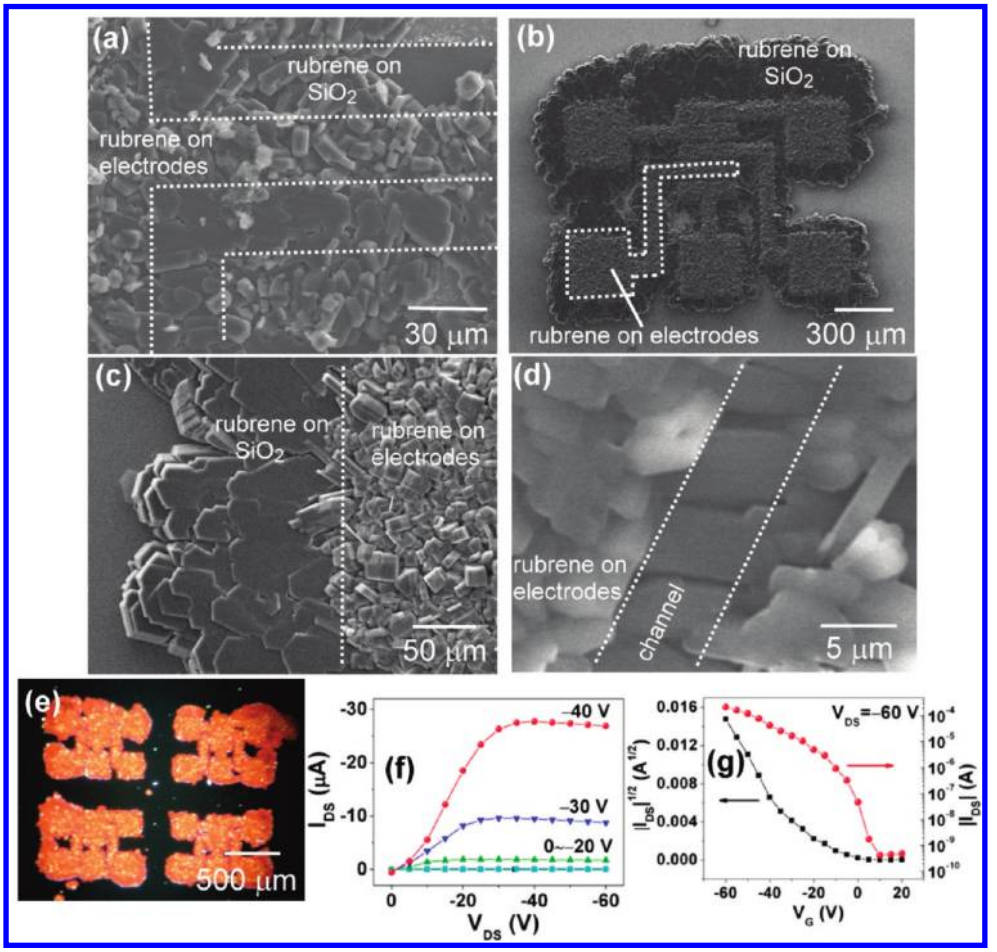


**Figure 4.** (a−c) SEM images of the patterned rubrene crystals. The source temperature is kept at 255 °C, and the substrate temperature is maintained at 170 °C (a) for 10 min and (b, c) 60 min. (d) SEM images of rubrene OFETs with short channel length; (e) optical micrograph of OFETs with patterned rubrene crystals; (f) output and (g) transfer characteristics of rubrene devices.

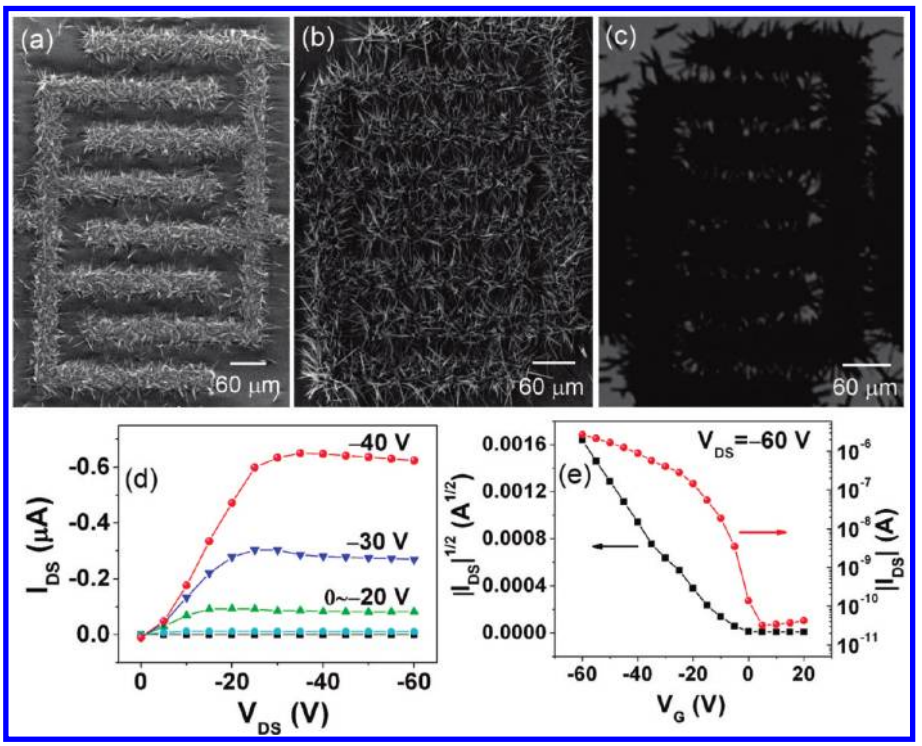


**Figure 5.** SEM images of CuPc crystals under different deposition conditions. The deposition temperature is kept at 415 °C and the substrate temperature is maintained at 260 °C for (a) 15 min and (b) 60 min. (c) Optical micrograph of OFETs with patterned CuPc crystals; (d) output and (e) transfer characteristics of CuPc OFETs.

the crystals tend to grow vertically to the electrode in the following deposition period. Figure 5b,c shows the SEM and optical micrograph images of CuPc devices after selective crystallization process, respectively. The needle-like CuPc crystals in the channel are well vertically patterned to the S−D electrodes (Figure 5). Similar with rubrene crystals, the CuPc crystals growing direction is consistent with the favorite carrier transport direction. The devices thus should possess good mobility in theory. However, CuPc devices exhibit very low mobilities of [$(1-5) \times 10^{-3}$ $cm^2/(V \cdot s)$]. This is due to poor contact between the dielectric layer and crystals. The problem does not exist for rubrene devices since the rubrene crystals grow next to the dielectric layer and the devices possess good dielectric/organic layer interface. Further improvement of dielectric/CuPc interface is undergoing to enhance the field-effect mobility.

To further investigate the relationship between the electrodes and the location of polycrystals, we fabricated OFETs with bare Au electrodes and bare Cu electrodes, respectively, without premodification of TCNQ. When Au serves as the electrodes, only a few crystals deposited on the substrate and no selective crystallization are observed for all of the three organic semiconductors. Similarly, no selective crystallization on bare Cu electrodes is observed after rubrene and CuPc deposition processes. Since only the devices with Cu-TCNQ-modified Cu electrodes can induce selective crystallization, the premodification of electrodes with Cu-TCNQ should be responsible for the selective crystallization of organic semiconductors.

There are two major characteristics of selective polycrystalline growth of organic semiconductors. First, all the crystals are located near the Cu-TCNQ-modified electrodes. Second, different organic semiconductors show varied crystallization paths, and the crystals tend to grow with the $\pi-\pi$ interaction direction vertical to the electrodes for rubrene and CuPc. We suggest the former phenomenon is determined by the crystal nucleation while the later one is related to crystal growth (Figure 6). According to classical nucleation theory, heterogeneous nucleation is driven by the interaction between the depositing semiconductors and the references therein. Note that, the interactions is greatest in the "valleys" between rough pillars and stabilizes the formation of a stable crystal.[24,26] As a result, heterogeneous nucleation are preferentially occur on rough surfaces than on the flat ones.[14,33] In these case, the nanosized Cu-TCNQ-modified electrodes provide a suitable surface for heterogeneous nucleation which thus induces crystal growth near the electrodes. The results prove once again that the rough surface induced nucleation and determined the selective polycrystalline of organic semiconductors.

Besides the location of the crystals, the different paths and direction of crystal growth are other interesting features. TCNQ crystals tend to grow on the electrodes, rubrene crystals prefer to extend into the channel easily,

(31) Seo, J. H.; Park, D. S.; Cho, S. W.; Kim, C. Y.; Jang, W. C.; Whang, C. N.; Yoo, K.-H.; Chang, G. S.; Pedersen, T.; Moewes, A.; Chae, K. H.; Cho, S. J. *Appl. Phys. Lett.* **2006**, *89*, 163505.
(32) Hara, K.; Tominari, Y.; Takeya *J. Mater. Res. Soc. Symp. Proc.* **2007**, *1003*, 38–40.
(33) Granasy, L.; Borzsonyi, T.; Pusztai, T. *Phys. Rev. Lett.* **2002**, *88*, 206105.

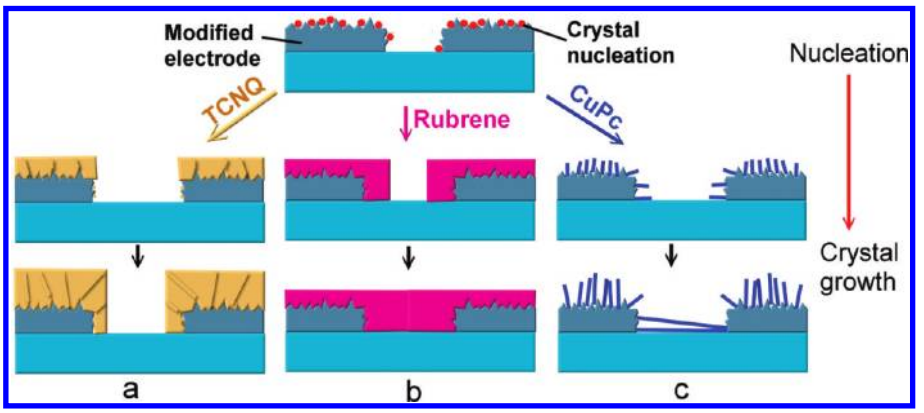


**Figure 6.** Illustration of selective crystals growth process: (a) TCNQ, (b) rubrene, and (c) CuPc.

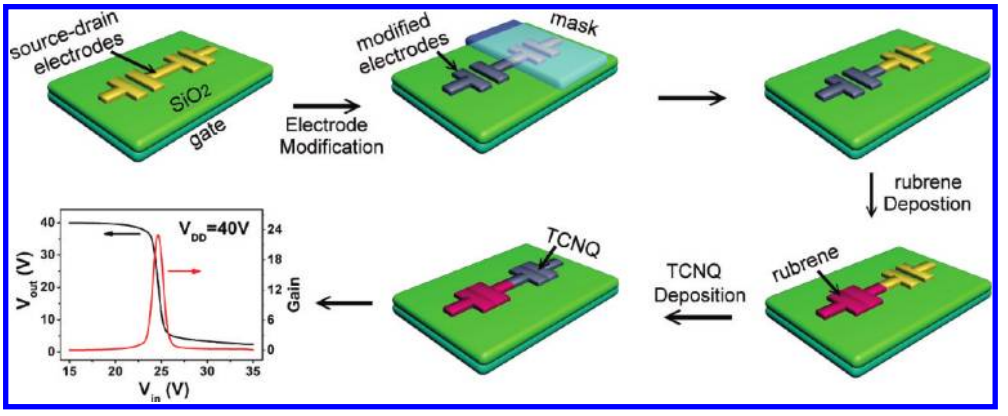


**Figure 7.** Scheme of fabrication process of organic inverter and transfer characteristics of a complementary inverter made of rubrene- and TCNQ-based OFETs. The inverter exhibits a maximum gain of 23.

while CuPc crystals are well vertically patterned to electrodes. Besides, for both rubrene and CuPc, the long sides of crystals are almost vertical to the electrodes which are favorable directions for carrier transport. We suggest the phenomenon is related to their molecule packing ways of the corresponding single crystals. TCNQ molecules in single crystals possess similar intermolecular interaction in three directions, which makes the crystals tend to grow in a 3D model. Therefore, the TCNQ crystals extend their width slowly together with the increase of thickness during the deposition process. Also, the Cu-TCNQ might possess strong interaction with TCNQ which could facilitate the growth of TCNQ crystals on the electrodes. As for rubrene, the single crystals grow in a 2D model. Here the crystals extend from the electrode in the horizontal direction and result in filled crystals near the electrodes. As far as crystal orientation control is concerned, a single crystal with the 1D growth model is more favorable. In the case of CuPc, the nucleation of the crystal formed is at the valley between the Cu-TCNQ nanocrystals. Due to strong CuPc intermolecular interaction ($\pi-\pi$ interaction) in a single direction, the crystals grow from the valley of electrodes with the direction of Cu-TCNQ nanowires, leading to the alignment of CuPc crystals. Consequently, the rough Cu-TCNQ modified electrode determined the nucleation position, while the crystal growth is dominated by the intermolecular interactions of organic semiconductors. Interestingly, the orientation control of organic crystals, a well-known challenge in this field, is partially resolved by our approach.

With the selective crystallization techniques, the fabrication of organic inverter in PVT system can be easily obtained. To illustrate its capability in organic circuits, we built inverter arrays with rubrene and TCNQ. Figure 7 shows the illustration of fabrication process of an inverter based on patterned OFETs. At first, the Cu electrodes are modified with a show mask to form partly Cu-TCNQ modified electrodes. Then, the device was placed into a PVT system to deposit rubrene and TCNQ, respectively. Thereafter, organic inverter based on patterned OFETs is constructed. It should be noted that, although TCNQ polycrystals deposit after the rubrene film formation without shadow mask, little TCNQ crystals deposit on rubrene films. The inverter exhibits good device characteristics with maximum gain larger than 20. The results demonstrate that our explored technique is a potential one for real application.

## Conclusions

In summary, we report on a novel approach to control selective growth of organic crystals and its application

in OFETs. Three different ways for crystal growth are investigated and are suggested to be related to the morphology of the electrodes and organic molecules' packing properties. These growth models could be used to realize location patterning of organic crystals, fabrication of high performance OFETs, and orientation control of organic crystals. By using rubrene as an organic layer, high field-effect mobility up to 4.6 $cm^2/(V \cdot s)$ is achieved. Therefore, the explored approach could serve as a novel method toward high performance OFETs with patterned polycrystals.

**Acknowledgment.** This work is supported by the National Natural Science Foundation of China (20825208, 60736004, 60671047, 50673093, 20721061), the Major State Basic Research Development Program (2006CB806203, 2006CB932103, 2009CB623603), the National High-Tech Research Development Program (2008AA03Z101), and the Chinese Academy of Sciences.